Understanding Microstructural Effects on Long Term Electrical Fatigue in Multilayer PZT Actuators*

Jens Müller[+,a], Stephanie A. Hooker[a], and Davor Balzar[a,b]
[a]Materials Reliability Division, National Institute of Standards & Technology (NIST), 325 Broadway, Boulder, CO 80305-3328
[b]Department of Physics and Astronomy, University of Denver, Denver, CO 80208

ABSTRACT

In this study, multilayered $PbTi_xZr_{1-x}O_3$ (PZT) samples were produced by tape-casting and subsequent sintering at temperatures in the range of 1175 °C to 1325 °C. Sintering times were 6 and 24 minutes. Samples were poled and additionally electrically fatigued by long-term exposure ($\approx 10^6$ cycles) to cyclic electric fields. The parameters of initial and remnant polarization were estimated from hysteresis loops. Changes in the crystallographic microstructure as a function of sintering temperature T_S were examined by scanning electron microscopy (SEM) and X-ray diffraction (XRD) to gain insight on fatigue mechanisms and their prevention. The microstructural results, such as domain reorientation and amount of secondary phases, explained the results of electrical observations. We found that grain sizes and internal strains were major influence factors on device performance. Domain wall movement was facilitated in samples processed at T_S less than 1250 °C, and such samples were more resistant to electrical fatigue. With increasing T_S, a tradeoff between higher device performance power and lower device degradation with usage time was observed.

Keywords: lead zirconate titanate, $PbTi_xZr_{1-x}O_3$ (PZT), electrical fatigue, sintering, XRD, SEM, domain size, grain size, domain reorientation

1. INTRODUCTION

The ongoing development of new applications that make use of piezoelectric ceramics, such as adaptive structures, vibration isolation, and nanorobotics, demands smaller, highly reliable and long-term use fatigue-resistant devices. Piezoelectric ceramics offer many desirable attributes for these applications, since they combine a fast response time with high achievable forces and a large power density. However, in order to achieve a maximum displacement in these instances, actuators will be operated with electric fields higher than those in conventional applications. Under such harsh driving conditions, an increased degradation in ferroelectric properties is observed. The decreasing device performance during long-term use is influenced by changes in the material's microstructure, such as domain pinning, relaxation of internal strains and the development of micro-cracks. Tailoring the ceramic microstructure by controlled sintering offers one possible route to improve fatigue resistance. Several further benefits can be achieved by the use of submicron-powdered materials. For instance, smaller particles allow a more intimate mixing of the basic materials, so possible flaws can be minimized already at the very beginning of the production process. In the past, an increased density of bulk devices showed to have positive effects on long term stability [1]. Additionally, submicron-powders can be sintered at lower temperatures. In this study, we examined how these benefits apply to actuator devices made from piezoceramic PZT submicron-powders, and to what extent microstructure control affects fatigue resistance.

2. EXPERIMENTAL DETAILS

2.1 Sample preparation

Samples were prepared by tape-casting from commercially available sub-micrometer sized powder of a soft composition (PZT-5A) [2], which was prepared by attrition milling for 6 hrs and possessed a particle size of about 140 nm. The material was mixed into a slurry and stacked, tacked and laminated before binder burn-out and firing. Platinum (Pt)

+ jmueller@boulder.nist.gov; phone 1 303 497-7065; fax 1 303 497-5030; www.nist.gov

electrodes embedded in the material between the layers had a spacing of 50 μm to 60 μm, as shown in Figure 2a. Each sample consisted of ten electrically active layers plus an additional inactive layer on top and bottom, respectively, resulting in a total sample thickness of about 0.9 mm (see Figure 1). Four different sample sets were examined in this study, as defined in Table 1. Every set consisted of seven samples, with each sample sintered at a different sintering temperature T_S, while buried in PZT powder. The samples of sets 1 to 3 were sintered for 24 minutes, while set 4 was sintered for only 6 minutes. Sintering temperatures ranged from 1175 °C to 1325 °C, with a ΔT of 25 ºC between samples.

Table 1 Overview of examined sample sets in this study. Each set consisted of seven samples. The first sample of a set was processed at 1175 °C. For each following sample the sintering temperature was increased 25 °C, up to 1325 °C for the last sample of a set. For poling, an electric DC field of 20 kV/cm was applied for 20 s. Electrical fatiguing was performed by application of an electric AC field with an amplitude of 15 kV/cm and a frequency of 35 Hz (sine wave). Typically a sample was fatigued for about 10^6 cycles.

Sample Set #	***1***	***2***	***3***	***4***
Electrical treatment	*as-produced*	*poled*	*poled & fatigued*	*as-produced*
Sintering time (minutes)	24	24	24	6

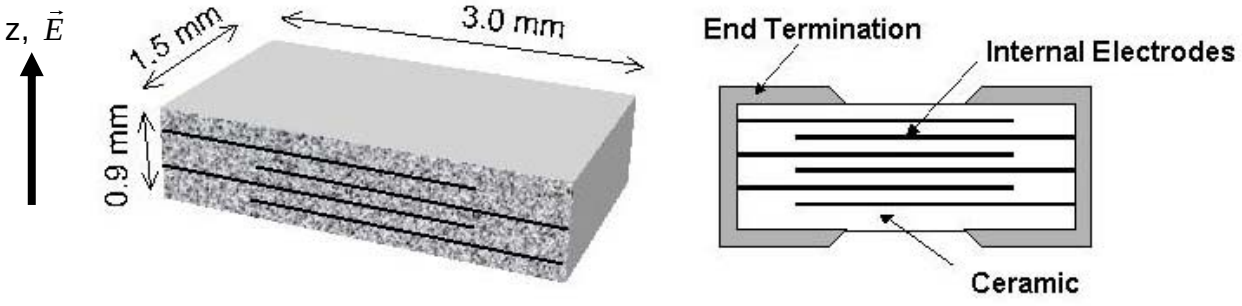

Figure 1 Schematic display of sample geometry. The external electrical AC and DC field vectors were oriented perpendicular to the sample surface.

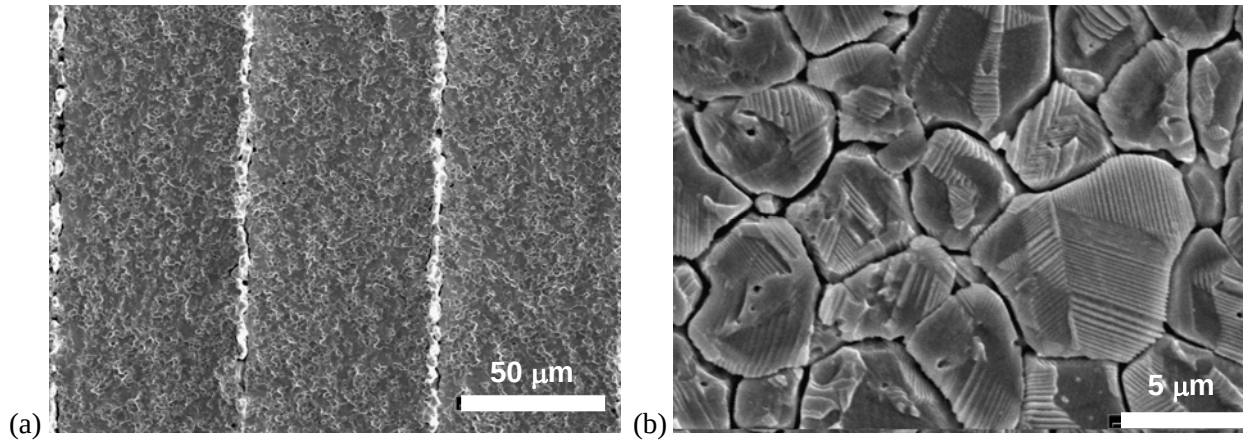

Figure 2 (a) SEM image of an unpolished cross-section. The thickness of an active layer (*i.e.*, the electrode spacing) is about 60 μm. (b) Domain- and grain-boundary structures, made visible in SEM by etching of a polished surface

The different sets are defined as follows: *Sets 1* and *4* are referred to as "as-produced", meaning that the only difference between the samples in these sets is T_S. The results of microstructure study obtained for this set were used as a reference to separate the influences of electric treatment on the microstructure for the samples of sets 2 and 3. *Set 2* was electrically poled after production, a process that is typically performed for actuators to achieve the necessary degree of domain orientation for optimum physical displacement.

2.2 Electrical treatment

During poling, a direct current (DC) electric field of 20 kV/cm was applied to the samples for 20 seconds along the *z*-axis (*i.e.* perpendicular to the sample's surface). In addition, *set 3* was electrically fatigued after poling. During this process, the samples were clamped along the end terminations (see Figure 1), and an alternating current (AC) electric field (35 Hz sine wave, 15 kV/cm) was applied for about 10^6 cycles to simulate long-term cyclic operation. This process fatigues the actuator, because the domains try to follow the external electric field by ferroelectric domain switching. However, with time, a reduction in switchable polarization is found due to electric stress (polarization fatigue), and domains may become pinned in one position. This accumulating effect can lead to electrically inactive sample volumes and dramatically decrease device performance. A more exhaustive overview of effects involved in polarization fatigue can be found in [4]. The polarization of a ferroelectric sample (the sum of polarization vectors aligned with the *z*-axis/external field direction) was estimated from measurements of ferroelectric hysteresis (polarization *vs.* electric field) with a Sawyer-Tower circuit. The remnant polarization P_r is defined as the remaining polarization that is still present in a material after the applied external electric field is removed (or equal to zero during hysteresis). P_r is a measure of the fraction of domains still able to switch. The polarization of a poled (but unfatigued) sample is called the initial polarization P_{init}.

2.3 SEM

In order to study the grain size by SEM as a function of T_S, as-produced samples were cross-sectioned and mechanically polished. To enhance the grain boundaries and domain structures, the cross-sections were subsequently etched with a water-diluted solution of hydrochloric and hydrofluoric acid [5], as can be seen in Figure 2b. To prevent charging during SEM analysis, a thin layer of gold was sputtered onto each surface prior to imaging. The determination of grain size was performed by the intercept method, with an average number of 300 counted grains per image.

2.4 XRD

To study the initial and fatigued domain orientation, XRD scans were acquired for the 2θ region 20º to 80° (Figure 4a) and in closer detail for 20º to 24° and 42º to 47°, which include the (001) and pseudocubic (002) peak region, respectively. The reflections observed in these ranges were attributed to the tetragonal, rhombohedral and monoclinic phase of PZT [6], as shown in Figure 4b and Figure 5. The term 'pseudocubic' arises from the fact that the differences between unit cells of these three phases are minor, and the lattice can be closely described by its cubic state. Additional reflections observed in longer range scans were attributed to the pyrochlore phase that formed at sintering temperatures above 1250 °C. From XRD scans, we extracted information about the size of coherently diffracting domains (CDD), the orientation of ferroelectric domains (FD), the lattice parameters a_0 and c_0 (determined by Cohen's least-square method [7]) and the amount of secondary phases from integrated peak intensities. The analysis of XRD data was carried out by use of freely available software [8]. Volume-weighted CDD sizes of the first three sample sets were determined from line-broadening analysis of the pure physically broadened profiles of the tetragonal (001) and (002) reflections, with the instrumental contribution removed numerically (a more detailed description can be found elsewhere [9]). The uncertainty of a fit was typically less than 5 %.

In this study, ferroelectric domains with their crystallographic *c*-axis (polar axis) perpendicular to the sample's surface are referred to as *c*-domains, which yielded the tetragonal (002) diffraction peak. Ferroelectric domains with their *c*-axis parallel to the sample's surface are referred to as *a*-domains, which yielded the tetragonal (200) diffraction peak. As the integrated area intensities $I_{(002)}$ and $I_{(200)}$ of these peaks are directly related to the population of *c*- and *a*-domains, the intensity ratio $I_{(002)}/I_{(200)}$ can be used to determine the orientation state of the material. The amount of *a*- and *c*-domains in terms of percentage can be calculated from

$$\%\ a\text{-domains} = 100 - 100 \cdot \frac{I_{(002)} / I_{(200)}}{I_{(002)} / I_{(200)} + 1} \quad , \tag{1}$$

$$\% \, c\text{-domains} = 100 \cdot \frac{I_{(002)} / I_{(200)}}{I_{(002)} / I_{(200)} + 1}. \quad (2)$$

Because in the tetragonal phase the lattice parameters a_0 and b_0 are indistinguishable, the value of intensity ratio $I_{(002)}/I_{(200)}$ of a randomly oriented material is 0.5, which yields 67 % *a*-domains and 33 % *c*-domains.

3. RESULTS AND DISCUSSION

3.1 Electrical measurements

As it can be seen in Figure 3a, the values of initial polarization P_{init} increase as a function of T_S, reaching a maximum of 26 μC/cm^2 near T_S = 1275 °C,. The results of polarization-fatigue are shown in Figure 3b. We found that the fractional change in P_r as a result of cyclic actuation was significantly smaller for samples processed at T_S < 1250 °C, indicating a higher fatigue resistance in this temperature range. However, a nearly constant level of fatigue (≈50 % of P_{init}) is found for T_S > 1250 °C (more detailed results of electrical polarization-fatigue measurements can be found elsewhere [10]). In the following, these electrical results will be explained by the observed changes in microstructure.

3.2 Microstructure

Estimated values of surface grain sizes t_{sur} of as-produced samples are shown in Table 2. Since the growth of grains is a time-dependent process, the smaller grain size values of sample set 4 are easily explained by the shorter sintering time of this set. The values of CDD size were similar to the ferroelectric domain sizes determined from SEM images. Because CDD sizes were approximately two orders of magnitude smaller than grain sizes, domain-grain wall interaction is not expected to impede the switching ability of domains in the examined actuators [11]. From the calculated lattice parameters c_0 and a_0 we found an increasing tetragonality c_0/a_0 of unit cells as a function of T_S for all samples, as can be found in Table 2.

Table 2 Estimated data of surface grain size t_{Sur}, volume weighted CDD size D_V and unit cell tetragonality c_0/a_0 of as-produced samples with sintering time of 24 minutes and 6 minutes (Sets 1 and 4)

T_S (ºC)	1175	1200	1225	1250	1275	1300	1325
	24 min (Set 1)						
t_{Sur} (μm)	2.2 ± 0.23	2.6 ± 0.52	2.9 ± 0.49	3.2 ± 0.50	3.6 ± 0.48	3.8 ± 0.46	3.7 ± 0.48
D_V (nm)	33 ± 7.6	72 ± 5.3	53 ± 9.6	51 ± 8.6	69 ± 17.9	84 ± 39.2	64 ± 21.3
c_0/a_0	1.019(6)	1.023(2)	1.024(6)	1.024(5)	1.025(7)	1.027(5)	1.028(4)
	6 min (Set 4)						
t_{Sur} (μm)	1.1 ± 0.12	1.3 ± 0.15	1.7 ± 0.13	2.4 ± 0.19	2.8 ± 0.24	3.2 ± 0.34	3.4 ± 0.40
c_0/a_0	1.017(8)	1.018(4)	1.021(9)	1.023(5)	1.019(1)	1.023(8)	1.021(9)

3.3 Domain orientation and secondary phases

Due to the minor differences in structure of PZT phases, it is likely to find amounts of secondary phases next to the main tetragonal phase. It can be seen in Figure 6b that in as-produced samples of set 1 the rhombohedral phase was present in varying amounts in the whole range of T_S. This caused a uniform distortion of the lattice that was evidenced by a split of the tetragonal (110) peak into two symmetrical doublets [12]. For fatigued samples a strong rhombohedral-to-tetragonal phase transition was observed for samples sintered near 1225 °C, as shown in Figure 6b. This indicates that the long-term ferroelectric switching of domains induced by the applied AC field causes rhombohedral unit cells to transform into the tetragonal phase to better align their polar axis with the electric field direction.

Another parameter that was strongly influenced by the AC and DC fields is the orientation distribution of domains. Figure 6a shows the population of *c*-domains, *i.e.*, domains oriented with their polarization along the electric field, for sample sets 1 to 3. For T_S < 1250 °C, as-produced samples exhibit a typical population of 33 % *c*-domains. For higher

sintering temperatures this population decreases to about 25 %, which is caused by an observed rise in intensity of the monoclinic (220) peak for T_S > 1250 °C. The shift to a more *a*-oriented domain distribution is caused by the small difference between monoclinic and tetragonal unit cells. As can be seen in Figure 5, the monoclinic (220) orientation is in principle a slightly distorted tetragonal (200) orientation. We found the amount of the monoclinic phase to be independent on T_S and only to depend on sintering time. Samples of the shorter sintered sample set 4 exhibited no monoclinic phase, even at highest T_S. As a result, the *c*-domain population of these samples did not vary with T_S. For the poled samples of set 2, we observed an expected increase in the population of *c*-domains (≈5 %) relative to the as-produced state, as shown in Figure 6a. The reason is that the applied DC field caused a 90º-domain switch of a certain amount of *a*-domains into *c*-orientation. However, the increase in *c*-domain population seemed to be independent of T_S and is nearly constant for all poled samples. Hence, the poling effect depended solely on the duration and strength of the applied DC field.

The most significant changes in microstructural properties were observed for the electrically fatigued samples. It can be seen in Figure 6a that compared to as-produced and poled samples, an increase in *c*-domain population is observed only for sintering temperatures below 1250 °C, while for higher temperatures the material shows no major difference in the domain population between poled and fatigued samples.

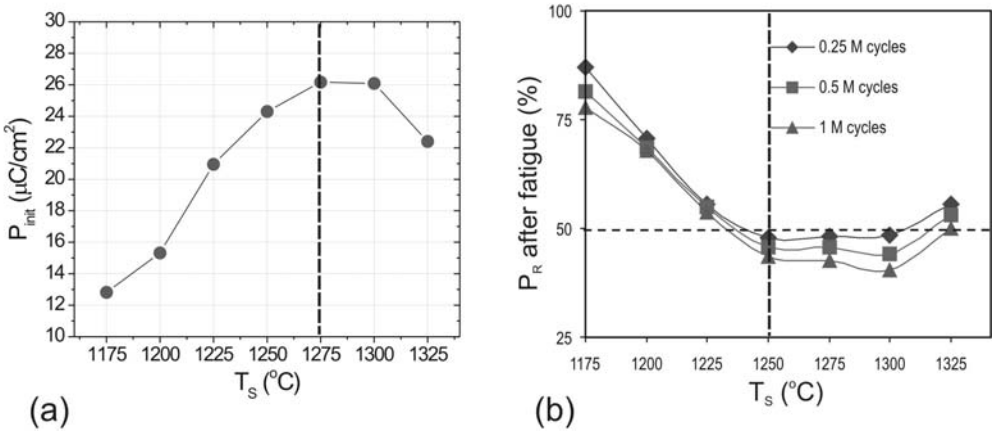

Figure 3. (a) Initial polarization P_{init} of poled samples (Set 2); (b) Remnant polarization P_R of fatigued samples (Set 3) in terms of percentage of P_{init};

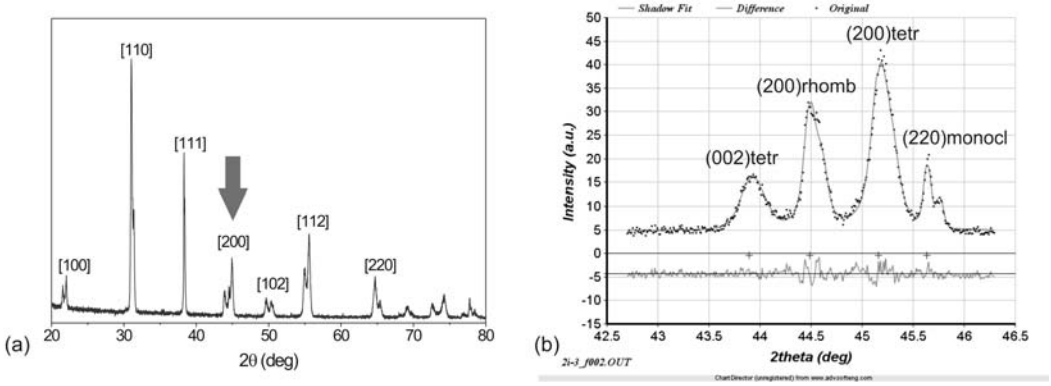

Figure 4 (a) Typical XRD scan of a PZT sample at lower T_S. (b) Due to the close neighborhood of reflections of the tetragonal, rhombohedral and monoclinic phase, the pseudocubic (200) region is of special interest.

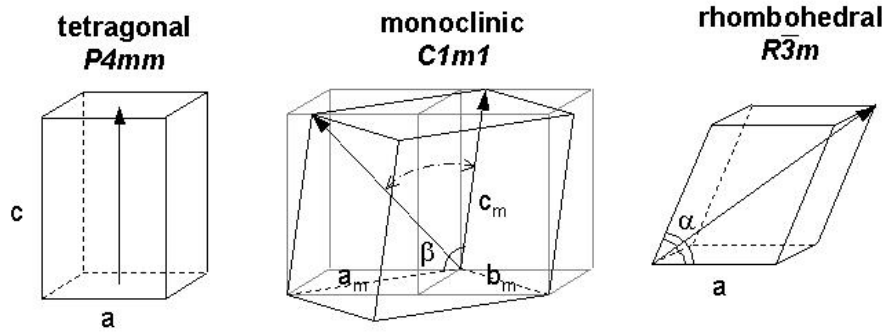

Figure 5 Schematic display of unit cells of individual phases of PZT. However, differences between the shown and the cubic phase of PZT are rather small.

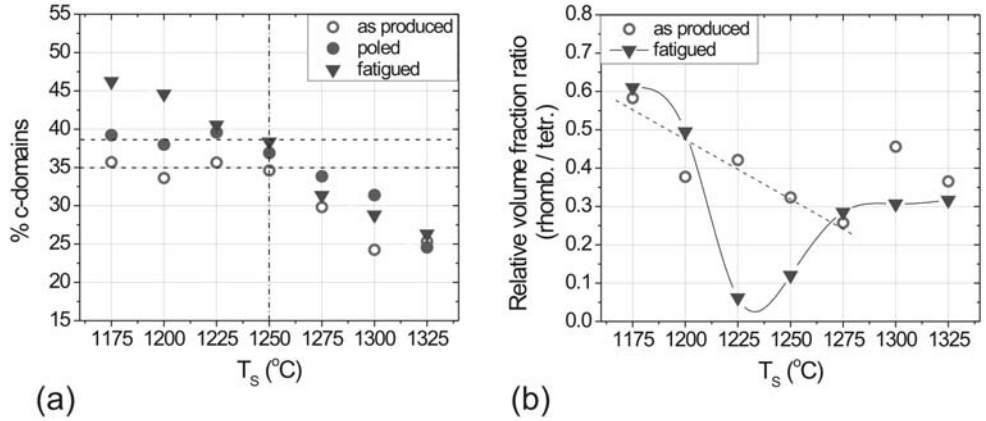

Figure 6. (a) Population of *c*-domains for sample sets 1 to 3, calculated from integrated XRD peak intensities; (b) Volume fraction of the rhombohedral phase in relation to the tetragonal phase (Sets 1 and 3), calculated from the ratio of integrated XRD peak intensities $I(200)_{rhomb} / [I(200)_{tetr} + I(002)_{tetr}]$

With these results in mind we now can explain the observed behavior of initial polarization P_{init} and remnant polarization P_R that are shown in Figure 3. For P_{init} two influencing factors were identified: *unit cell tetragonality* and *population of c-domains*. According to XRD measurements, the tetragonality of both *a*- and *c*-oriented unit cells increased over the whole temperature range (thus increasing the length of polarization vectors). However, for $T_S > 1250$ °C an increasing amount of material preferred to grow in the (220)-oriented monoclinic phase (distorted tetragonal *a*-orientation) instead of the (002)- oriented tetragonal phase. The resulting decrease in the population of tetragonal *c*-domains causes the observed drop in P_{init} at high T_S. It has to be kept in mind that only movable ("active") *c*-oriented domains contribute to the observed polarization. The change in active *c*-domains with each field cycle can be expressed as

$$\Delta\%\ c\text{-domains}(T_S, cycle\#) \sim p_{pin}(T_S, cycle\#) \cdot p_{switch}(T_S, cycle\#), \quad (3)$$

with

cycle# : Number of performed hysteresis loops during electrical fatiguing

p_{pin} : Probability per field cycle for a *c*-domain to become pinned; depends on the amount of domain wall movement-impeding effects (such as secondary phases and lattice defects); increases as a function of T_S and cycle number.

p_{switch} : Probability per field cycle for an AC-field induced *a*- to *c*-domain switch to release strain; determined by the level of clamping strain and the number of available *a*-domains; decreases as a function of T_S and cycle number.

Therefore, because p_{pin} is small and p_{switch} is big at lower T_S, the number of activated *a*-domains will surpass the number of pinned *c*-domains in this temperature range. The constant values of P_R that are found in the higher T_S-range are consistent with the microstructural result that for $T_S > 1225$ °C no reorientation of domains is observed in comparison to the poled state, as shown in Figure 6a. This indicates that the mobility of domain walls no longer varies with T_S in this temperature range. Due to domain wall movement impeding factors, *c*-domains are pinned early in the fatiguing process and a replacement by activation of *a*-domains is less probable.

4. SUMMARY

PZT actuators were produced by tape-casting of submicron powder material and subsequent sintering at temperatures T_S in the range of 1175 °C to 1325 °C. The typical sintering time was 24 minutes, and 6 minutes for some additional samples. Some samples were poled and electrically fatigued for about 10^6 cycles. Changes in microstructure as a function of T_S, poling and electrical fatigue were examined with SEM and XRD. SEM images of cross sections yielded grain sizes that ranged from 1.1 µm to 3.8 µm, depending on T_S and sintering time. Volume-weighted coherently diffracting domain sizes, calculated by XRD line broadening analysis, were 20 nm to 80 nm and comparable to ferroelectric domain sizes estimated from SEM images. An examination of integrated XRD peak intensities showed that the rhombohedral phase was always present in varying amounts. The monoclinic phase only arose for $T_S > 1250$ °C, shifting the original uniform orientation distribution of ferroelectric domains towards more *a*-oriented (up to 14 % fewer *c*-domains). Samples sintered for only 6 minutes exhibited no monoclinic phase amounts, indicating that the build-up of this phase was time-dependent. Poled samples showed an increase in ferroelectric *c*-domain population in comparison to the as-produced state, due to polarization alignment of *a*-domains with the external DC field by switching into *c*-orientation.

The results of microstructural measurements explain the observed behavior of initial and remnant polarization, evaluated from electrical hysteresis plots. An increasing initial polarization P_{init} as a function of T_S was found that was influenced by unit cell tetragonality and ferroelectric *c*-domain population. On the other hand, a higher fatigue resistance was observed for samples processed at $T_S < 1250$ °C, where samples possessed still up to 75 % of their initial polarization after fatiguing. Those samples that were most fatigue resistant also showed a distinct increase in *c*-orientation in comparison to the poled state. This behavior was caused by an increased probability per field cycle for inactive *a*-domains to switch into *c*-orientation, where they would contribute to the observed polarization. The switching probability was influenced by factors such as internal strain and the amount of lattice defects and secondary phases. The strain referred to was likely caused by a clamping of the spontaneous tetragonal distortion of PZT by smaller grain sizes in the low sintering temperature region. This left the material in a compressively strained state and made the *c*-orientation of domains energetically more favorable, since here the external electric field increased the unit cell tetragonality and helped to reduce strain. For $T_S > 1250$ °C the population distribution of ferroelectric *c*- and *a*-domains was nearly identical for poled and fatigued samples, indicating an increased impediment of domain wall movement and faster pinning of domains.

Therefore, a tradeoff was observed between higher device performance power for $T_S > 1250$ °C and lower device degradation with usage time for $T_S < 1250$ °C. Future investigations will deal with the improvement of initial polarization at lower T_S.

REFERENCES

[1] Q. Jiang, and L. E. Cross, “Effect of porosity on electric. fatigue behavior in PLZT and PZT ceramics”, J. Mater. Sci. **28**, 4536 (1993).

[2] H. Pölzl, and E. Brzozowski, CFI-Ceram. Forum Int. **82**(4), E37 (2005).

[3] http://piezocenter.com/standardmaterial.htm (2005).

[4] A. K. Tagantsev, I. Stolichnov, E. L. Colla, and N. Setter, “Polarization fatigue in ferroelectric films: Basic experimental findings, phenomenological scenarios, and microscopic features”, J. Appl. Phys. **90**(3), 1387 (2001).

[5] U. Täffner, V. Carle, and U. Schäfer, ASM Handbook Volume 9: Metallography and Microstructures, ASM International, Materials Park, OH (2004).

[6] ICSD Data Base Entry, Pb(Zr0.52Ti0.48)O3-[P4MM] R. Ragini, R. Ranjan, and S. K. Mishra, http://icsdweb.fiz-karlsruhe.de (2002).
[7] M. U. Cohen, "Precision Lattice Constants from X-Ray Powder Photographs", Rev. Sci. Instr. **6**, 68 (1935).
[8] D. Balzar, *J. Appl. Cryst.* **28**, 244 (1995). Programs SHADOW, SLH, and BREADTH are available from http://www.du.edu/~balzar/lbap.htm.
[9] D. Balzar in *Defect and Microstructure Analysis by Diffraction*, edited by R. L. Snyder, H. J. Bunge, and J. Fiala, (International Union of Crystallography Monographs on Crystallography **No. 10**, Oxford University Press, New York 1999) pp. 94.
[10] S. Hooker, J. Müller, C. Kostelecky, and K. Womer, *Journal of Intelligent Material Systems and Structures*, (accepted for publication July 2005).
[11] C. A. Randall, N. Kim, J. P. Kucera, W. Cao, and T. R. Shrout, "Intrinsic and Extrinsic Size Effects in Fine-Grained Morphotropic-Phase-Boundary Lead Zirconate Titanate Ceramics", J. Am. Ceram. Soc. **81**(3), 667 (1998).
[12] C. N. Darlington, and R. J. Cernik, "Synchrotron X-ray powder diffraction study of $(Pb_{1-3x/2}La_x)$ $(Zr_yTi_{1-y})O_3$ at elevated temperatures", J. Phys.: Condens. Matter **1**, 6019 (1989).
[13] Y. Fotinich, and G. P. Carman, "Stresses in piezoceramics undergoing polarization switchings", J. Appl. Phys. **88**(11), 6715 (2000).